Nano Research 2018, 11(12): 6141–6154
https://doi.org/10.1007/s12274-018-1971-6
Research Article
ISSN 1998-0124
CN 11-5974/O4

Versatile multiplexed super-resolution imaging of nanostructures by Quencher-Exchange-PAINT

Tobias Lutz[1], Alexander H. Clowsley[1], Ruisheng Lin[1], Stefano Pagliara[1], Lorenzo Di Michele[2], and Christian Soeller[1] (✉)

[1] *Living Systems Institute & Biomedical Physics, University of Exeter, Exeter EX4 4QD, UK*
[2] *Cavendish Laboratory, University of Cambridge, Cambridge CB3 0HE, UK*

Received: 12 October 2017
Revised: 20 December 2017
Accepted: 21 December 2017

KEYWORDS
super-resolution microscopy,
fluorescence imaging,
DNA nanotechnology,
DNA-PAINT,
fluorescence quencher

ABSTRACT

The optical super-resolution technique DNA-PAINT (Point Accumulation Imaging in Nanoscale Topography) provides a flexible way to achieve imaging of nanoscale structures at ~ 10-nanometer resolution. In DNA-PAINT, fluorescently labeled DNA "imager" strands bind transiently and with high specificity to complementary target "docking" strands anchored to the structure of interest. The localization of single binding events enables the assembly of a super-resolution image, and this approach effectively circumvents photobleaching. The solution exchange of imager strands is the basis of Exchange-PAINT, which enables multiplexed imaging that avoids chromatic aberrations. Fluid exchange during imaging typically requires specialized chambers or washes, which can disturb the sample. Additionally, diffusional washout of imager strands is slow in thick samples such as biological tissue slices. Here, we introduce Quencher-Exchange-PAINT—a new approach to Exchange-PAINT in regular open-top imaging chambers—which overcomes the comparatively slow imager strand switching via diffusional imager washout. Quencher-Exchange-PAINT uses "quencher" strands, i.e., oligonucleotides that prevent the imager from binding to the targets, to rapidly reduce unwanted single-stranded imager concentrations to negligible levels, decoupled from the absolute imager concentration. The quencher strands contain an effective dye quencher that reduces the fluorescence of quenched imager strands to negligible levels. We characterized Quencher-Exchange-PAINT when applied to synthetic, cellular, and thick tissue samples. Quencher-Exchange-PAINT opens the way for efficient multiplexed imaging of complex nanostructures, e.g., in thick tissues, without the need for washing steps.

1 Introduction

With a wide range of requirements for optical imaging in molecular biology and medicine, a broad spectrum of different techniques have emerged, with many recent ones allowing for the imaging of structures

Address correspondence to c.soeller@exeter.ac.uk

smaller than the diffraction limit of light [1, 2]. Examples include structured illumination microscopy (SIM) [3], 4Pi [4], stimulated emission depletion (STED) microscopy [5, 6], (fluorescence) photoactivated localization microscopy [(F)PALM] [7, 8], (direct) stochastic optical reconstruction microscopy [(d)STORM] [9, 10], and combinations of different methods [11, 12].

The relatively straightforward-to-implement method DNA-PAINT (Point Accumulation Imaging in Nanoscale Topography [13]) is based on transient binding of fluorescently labeled oligonucleotides [14, 15]. Although labeled strands ("imager") in solution are detected only as a diffuse fluorescence background signal, they appear as diffraction-limited spots once they bind to a complementary target strand ("docking strand") as a result of the transient immobilization and can be localized with single-nanometer precision. The diffuse background can be minimized by imaging in total internal reflection fluorescence (TIRF) or highly inclined and laminated optical sheet (HILO) modes and binding times can be adjusted by modifying buffer conditions and strand lengths. This approach enables imaging with high specificity and contrast and, unlike other super-resolution techniques, dye photobleaching is negligible.

Because the fluorescent marker is not fixed on the target structure, multiplexed imaging can be achieved by exchanging imager solutions with different sequences, a method known as Exchange-PAINT [14, 16, 17]. This imaging of multiple targets with Exchange-PAINT by means of the same fluorescent dye gives an image free of chromatic aberrations. Nonetheless, current Exchange-PAINT protocols require lengthy washing steps and potentially complex fluidics systems. Especially in samples with limited diffusion, e.g., tissue slices, the switching time between different imagers can be substantial due to slow diffusional removal of imagers. The washing steps are critical because full removal of imagers between exchange rounds is crucial for crosstalk-free imaging.

Here, we demonstrate imager switching by a revised and simplified procedure, called Quencher-Exchange-PAINT. Instead of washing off and replacing imager strands, we add so-called "quencher strands," which hybridize to, and thus passivate, the imager. This action rapidly reduces the effective concentration of free single-stranded imagers available for binding with docking strands. To maintain a low fluorescent background, a fluorescence quencher is conjugated to the quencher strand, with minimum intramolecular distance to the imager dye. We show that the use of quencher strands allows for easier sequential target imaging without the need for washing steps or specialized chambers. Quencher-Exchange-PAINT imaging can be performed in a conventional open-top imaging chamber, and imager binding to the docking strand is rapidly stopped by adding a small volume of quencher strands at a sufficiently high concentration into the imaging chamber.

We show that a suitably designed quencher–imager pair with high affinity enables short switching times, up to an order of magnitude shorter than conventional Exchange-PAINT does, while yielding the same imaging quality. Furthermore, imaging of nanostructures in tissue slices with rapid imager switching is demonstrated. Switching is decoupled from the slow, diffusion-limited imager removal from the sample during imaging of a tissue slice because the concentration of quencher strands rises to a level required for inhibition more rapidly in comparison with the diffusional removal of imagers at a washing step with a buffer solution.

2 Results and discussion

2.1 Tuning of the DNA-PAINT event rate with competitive strands

Binding-event rate optimization is crucial for efficient DNA-PAINT imaging [15, 16]. If too many binding events per frame are observed, the risk of overlapping events increases, reducing the localization precision. If the rate is too low, then imaging takes an unnecessarily long time. Exchange-PAINT represents an extreme case, in which the event rate has to be reduced to background levels before switching to a new round of imagers to ensure crosstalk-free imaging. The most obvious way to tune the binding-event rate during image acquisition is by changing the concentration of free imager strands. Usually, this task is accomplished by diluting or concentrating the imager strands in a microscope chamber (Fig. 1, top) during a sequence of washing steps; this approach directly changes the

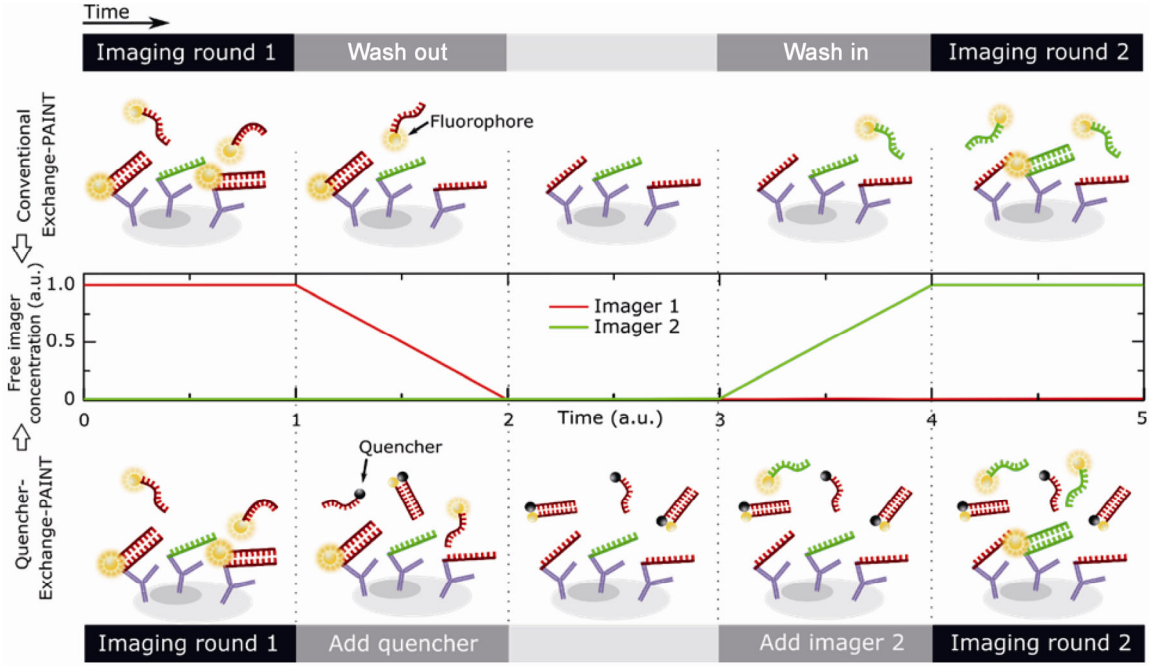

Figure 1 A sketch demonstrating conventional tuning of DNA-PAINT imager/docking binding-event rate vs. proposed tuning via quencher strands, which are complementary to the imager and thus compete with docking strands for binding to the imager. In DNA-PAINT, the event rate is proportional to the concentration of free imager strands. The concentration of free imager strands can either be tuned by the absolute concentration of the imager ("Conventional", top) or by adding a competitive complementary strand ("Quencher", bottom). The fluorescent quencher, conjugated to the competitive strand, reduces background fluorescence levels thus enhancing the signal-to-background ratio. In the schematic, the color of DNA strands identifies corresponding complementary strands, docking and imager strands 1 (red), docking and imager strands 2 (green).

event rate. Here, we propose Quencher-Exchange-PAINT, a scheme in which the free imager concentration can be reduced by simply adding a DNA strand complementary to the imager. The added complementary strand competes with the docking strand for binding to the imager. Fluorescence quenchers are conjugated to the competitive strand (which we therefore call a "quencher strand", see Fig. 1, bottom) to reduce background fluorescence and maintain a high signal-to-background ratio.

2.2 Design of an effective imager-and-quenching strand pair

It is desirable to minimize the concentration of competing binding strands required to significantly reduce free imager concentrations. The reason is two-fold: (1) This approach makes it practical to add only small amounts of a quencher strand solution to achieve fast and complete termination of docking-imager binding events, and (2) it reduces the concentration of the quencher strand in solution required to achieve essentially complete removal of free imagers. With respect to the latter consideration, tuning of the binding-event rate may be possible with a competitive complementary strand lacking a conjugated quencher. Nevertheless, this approach may come at the cost of significant background fluorescence from imagers that do not contribute to the super-resolution image, and this background in turn negatively affects localization precision [18]. This problem can be effectively avoided by addition of a quencher dye that quenches the fluorescence of competitively bound imagers, thereby maintaining a high signal-to-background ratio and high localization precision. On the other hand, extremely high quencher concentrations (> 10 μM) give rise to their own backgrounds as we show below, thus necessitating the design of a quencher–imager pair with high mutual affinity.

Efficient extinction of the imager dye fluorescence by the quencher is highly desirable. This notion was tested with long complementary strands that bind permanently and are labeled with a dye–quencher pair

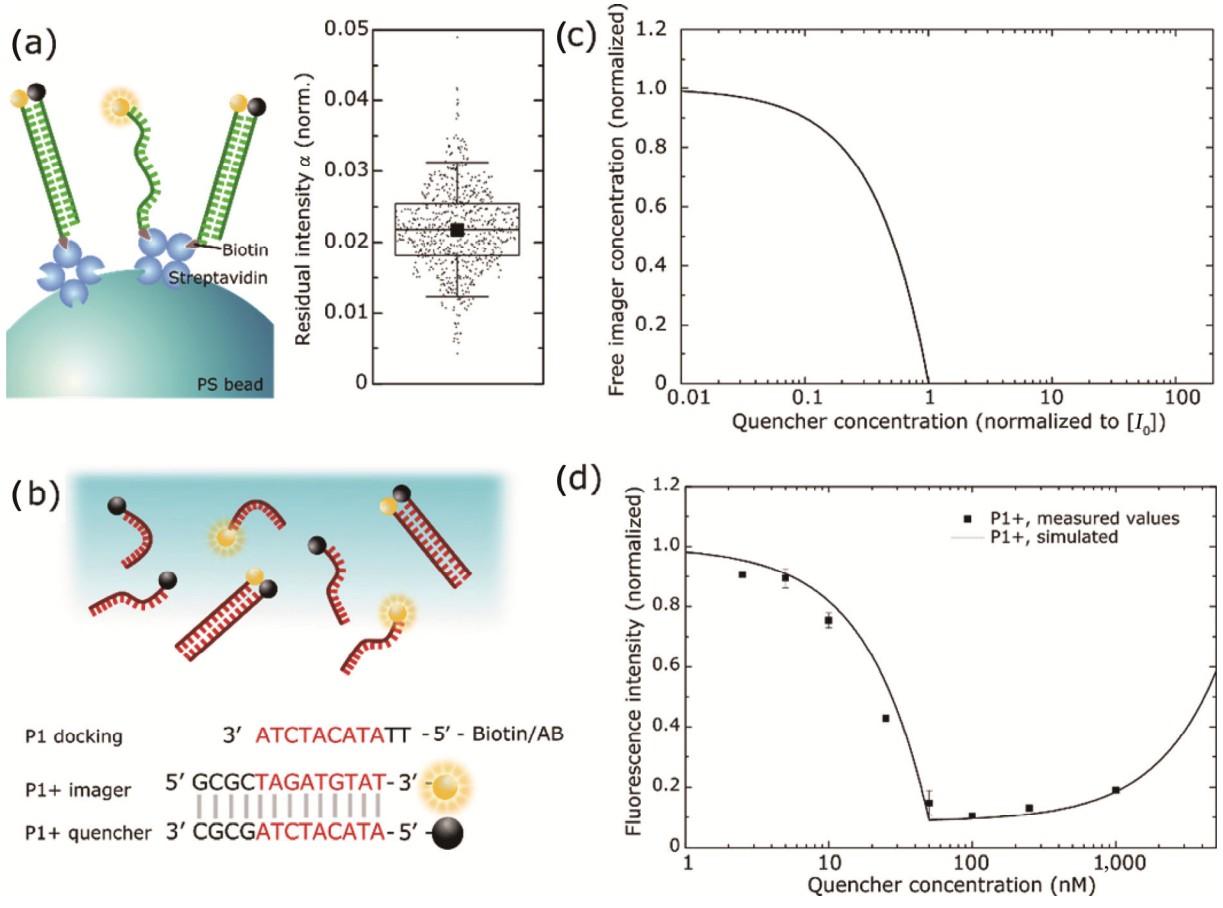

Figure 2 Quenching efficacy of a quencher coupled to complimentary oligonucleotides. (a) Dye-labeled, biotinylated oligonucleotides are linked to a streptavidin-coated polystyrene bead (bottom). Complementary quencher-modified strands (17 bp) will permanently bind, and the unbound quencher in solution is removed by washing. The residual fluorescence intensity per bead after saturated, permanent binding of quencher strands is 2.1% ± 0.6%. (b) Imager–quencher pair P1+ and complementary P1 docking strand used in (c) and (d). The sketch shows P1+ pairs bound and unbound in solution. (c) Modeled free imager concentration [*I*] for an imager–quencher pair with high binding affinity (P1+). (d) Experimental data on bulk fluorescence intensity for the imager–quencher pair, at an imager concentration of 50 nM. Line: modeled bulk fluorescence intensity. A rise of intensity for higher concentrations of the quencher owing to fluorescence of the quencher. Simulated fluorescence intensities with parameters $\alpha = 0.02$, $\beta = 5 \times 10^{-3}$, $\gamma = 0.07$, $K_d = 3.8 \times 10^{-5}$ nM at equilibrium. K_d was calculated with estimated $\Delta G = -18.0$ kcal·mol^{-1} (DINAmelt webserver [19, 20]).

(Atto 655 and Iowa Black RQ, Fig. 2(a)). Streptavidin-coated polystyrene beads were attached to a coverslip to act as anchors for biotinylated single-stranded DNA with a conjugated dye molecule. Complementary quencher strands with an overlap of 17 bp were added to the solution surrounding the beads, hybridized to the dye-labeled strands attached to the beads, and remaining free quencher and imager strands were washed out with plain buffer (see Experimental). The bulk fluorescence measurements indicated that fluorescence of the Atto 655 dye was reduced by approximately 98% upon hybridization with a quencher strand.

Criteria (1) and (2) above can be optimally fulfilled when quencher and imager strands have high binding affinity for each other, but the design must also ensure comparatively low affinity for transient binding between docking and imager strands; this condition is the basis of DNA-PAINT super-resolution.

On the basis of these considerations, we designed an imager–quencher pair using a DNA sequence termed P1+ (Fig. 2(b)), which is based on a previously published P1 design [14] but with a higher binding affinity as compared to the P1+ imager and P1 docking binding owing to an increased number (13) of complimentary bases between the P1+ imager and P1+ quencher. For this design, $\Delta G = -18.0$ kcal·mol^{-1} (under typical DNA-PAINT imaging buffer conditions, calculated with DINAmelt [19, 20] for 500 mM NaCl,

T = 293.15 K), so that dissociation constant $K_{d,q}$ becomes small enough (38.1 fM) to ensure near-permanent binding within the imager–quencher complex. The modeled curve based on equilibrium binding in Fig. 2(c) (for details see Electronic Supplementary Material (ESM), supplementary theory) indicates that the free imager concentration can be reduced to negligible levels once quencher strand concentration exceeds the imager concentration. Imaging quality is not expected to change relative to conventional DNA-PAINT because the transient low-affinity binding between the P1+ imager and the P1 docking strand involves only 9 complementary base pairs.

To estimate the background fluorescence intensity F, the residual fluorescence of a hybridized imager–quencher complex (IQ) as well as the fluorescence from the free quencher strand itself (Q) have to be taken into account. The background fluorescence should be proportional to the concentration of these species

$$F \propto [I] + \alpha[\mathrm{IQ}] + \beta[Q] + \gamma \quad (1)$$

where α and β are parameters that denote the ratio of fluorescence from quencher–imager complexes and quencher strands, respectively, versus a free imager strand; γ quantifies a nonspecific background that tends to be present in experiments; for details see Supplementary theory Eqs. (S1)–(S3) in the ESM. A curve calculated from this model is shown in Fig. 2(d) as a function of quencher strand concentration. Once the quencher concentration is much higher than the total imager concentration [I_0], the very small fluorescence of the quencher itself becomes non-negligible, and the total measured fluorescence increases.

The predicted dependence of fluorescence intensity based on model Eq. (1) was confirmed experimentally (Fig. 2(d), squares). Increasing concentrations of P1+ quencher strands were added to an imager present at a fixed concentration of I_0 = 50 nM, and bulk fluorescence F was recorded. The data showed that efficient quenching is possible with the quasi-permanently binding quencher strands and overcomes the limitations of a standard DNA-PAINT experiment. Notably, the measured fluorescence remains low from a quencher concentration of 50 nM up to several hundred nM, i.e., the fluorescence of the quencher is still negligible even at a 10× higher concentration of quencher strands compared to the imager concentration.

2.3 Tuning of the binding-event rate and background fluorescence by quencher strands

The anticipated reduction in background fluorescence by an imager–quencher pair with high binding affinity compared to the imager-docking binding affinity was tested in a Quencher-DNA-PAINT experiment as shown in Fig. 3. The extended imager sequence P1+ shows—just as the conventional imager P1—comparatively low affinity for transient binding between docking and imager strands because it contains the 9-base sequence of P1 to allow for transient binding to a P1 docking strand. Adding the quasi-permanently binding P1+ quencher strand to a solution containing the P1+ imager in DNA-PAINT tuned the effective concentration of the free imager. Here, we imaged 500-nm streptavidin-coated polystyrene beads that were labeled with biotinylated P1 docking strands and compared both the binding-event rate and the fluorescence background as a function of the effective free imager concentration [I]. If no quencher was added, then the free imager concentration equals the total imager concentration [I] = [I_0], and the binding-event rate increases proportionally to an increase in [I] (Fig. 3, black filled squares). Similar proportionality of the event rate with the effective free imager concentration is observed with added high-affinity P1+ quencher strands (Fig. 3, black empty squares), where [I] can be approximated as follows (see Supplementary theory Eq. (S4) in the ESM)

$$[I] \approx [I_0] - [Q_0] \quad (2)$$

As expected, the measured fluorescence background shows an approximately linear increase with the increasing total imager concentration in the absence of quencher strands (Fig. 3, red filled squares). If a quencher is added, and the measured background fluorescence is plotted against the remaining free imager concentration (calculated as [I_0] – [Q_0]), then a similar dependence is observed although the background is slightly higher (Fig. 3, red empty squares). This result is consistent with residual fluorescence of the imager–quencher complex and free quencher itself (i.e., α, β > 0 in Eq. (1)). Overall, Fig. 3 shows that the

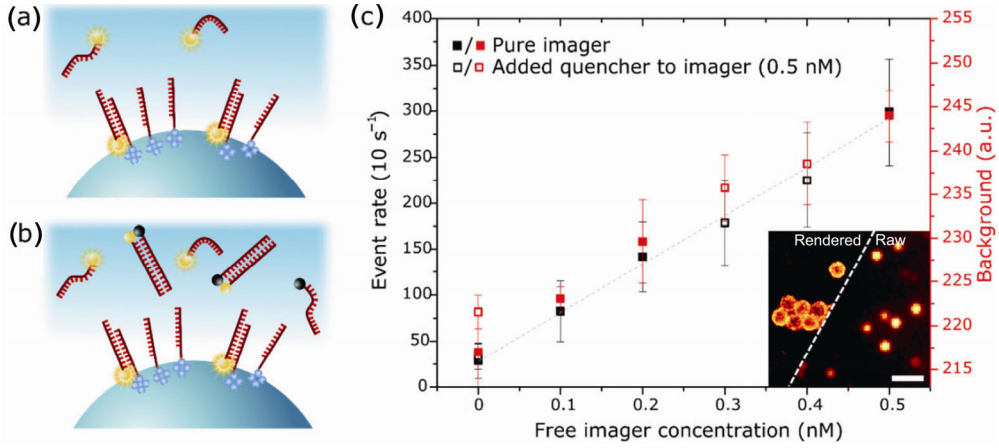

Figure 3 The effect of increasing imager and quencher concentrations on the DNA-PAINT event rate and fluorescence background. (a) The binding event rate of imager strands to docking strands attached to polystyrene beads is proportional to the concentration of unbound free imager strands. (b) The same effective free imager concentration, i.e., event rate, as in (a) can be achieved at a higher concentration of the imager, if the additional imager strands are bound to complimentary quencher strands. (c) Black: The event rate is proportional to the effective free imager concentration both without the quencher (filled symbols) and as the quencher concentration is varied with a fixed total imager concentration of 1 nM (empty symbols). The free imager concentration is estimated from equilibrium binding and K_d of 3.8×10^{-14} M. Inset: raw data and a rendered image of DNA-PAINT with polystyrene beads. Scale bar: 1 μm. Red: fluorescent background intensity after subtraction of the imager-unrelated offset increases linearly with the free imager concentration. With the added quencher (empty symbols), the background is generally higher than with an equivalent pure imager concentration at the same effective free imager concentration.

effective free imager concentration can be reduced both by adding the high-affinity P1+ quencher strand or by reducing the absolute imager concentration, resulting in a similar behavior of both the fluorescence background and the binding-event rate.

The experiments above showed that the use of the high-affinity quencher strands works as desired, namely, that the addition of the quencher strands in solution has an effect almost exactly equivalent to physical removal of imagers from the solution. This pattern holds both for the reduced pool of free imagers (that can bind to docking strands and thus reduce the binding-event rate by competitive binding) and for the reduction of bulk fluorescence by adding a fluorescence quencher modification to the quencher strand.

These findings also indicate that the use of quenchers is not suitable for increasing the signal-to-background ratio in DNA-PAINT, at least with simple competitive-binding strategies. The concomitant reduction in the event rate at best matches the reduction in the fluorescence background. In other words, one cannot do better in terms of the signal-to-background ratio for DNA-PAINT than adjusting imager concentrations to achieve the desired event rate, at least not via simple competitive quencher binding schemes. This list includes the quencher strand designs shown in this manuscript and extends to the potential use of molecular beacon imagers [21]. Nevertheless, the use of quenchers shown here is a practical alternative to actually removing imagers from the solution as we further demonstrate below in experiments with biological samples.

2.4 Quencher-Exchange-PAINT without the need for solution exchange

The presented high-affinity quencher/imager tuning scheme (as illustrated with the P1+ design) can be employed to implement Exchange-PAINT, that is, imaging serially with different imagers, without solution exchange. DNA-PAINT imaging of polystyrene beads (Fig. S1 in the ESM) and microtubules in fixed COS-7 cells (Figs. 4(a) and 4(b)) confirmed that the additional three bases of the P1+ imager sequence beyond those complementary to the P1 imager did not interfere with the imaging performance, because the docking-imager binding site was left unchanged. In rendered images, the localization error and the photon number per binding event yielded similar results with P1+ and P1 imagers.

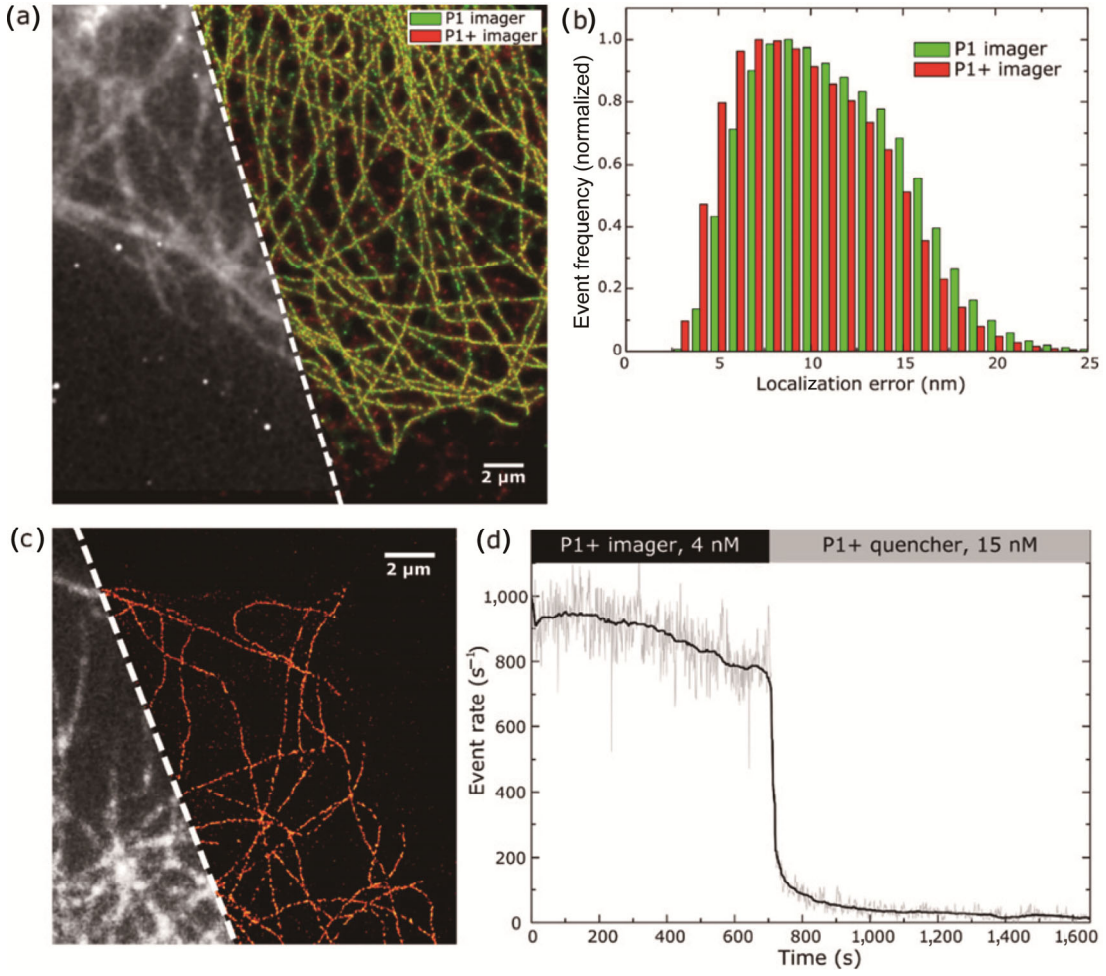

Figure 4 Efficient quenching of a modified imager strand with a quasi-permanently binding quencher shown on tubulin in fixed COS-7 cells. (a) DNA-PAINT imaging with a 10-base P1 imager (green) gives imaging quality similar to that of an extended 13-base P1+ imager (red). Grey: a fluorescent widefield image. (b) Similar localization errors for the P1 and P1+ imager confirm a similar binding behavior. The image shown in (a) rendering only localization events with an error < 8 nm. (c) Tubulin imaged for data shown in (d); grey: a fluorescent widefield image. (d) The localization event rate of tubulin imaged with the P1+ imager at 4 nM in an open chamber. At t = 710 s, 7.5 μL of the P1+ quencher is added to the 500-μL chamber to achieve a total quencher concentration of 15 nM. Efficient suppression of the binding-event rate can be achieved without washing or fluid exchange steps and without a high concentration of a quencher.

To demonstrate Quencher-Exchange-PAINT without the need for exchanging solutions, microtubules were imaged in an open-top chamber with a P1+ imager.

A small amount of concentrated complementary quencher strands was then added into the imaging chamber: Here, 7.5 μL of 1 μM P1+ quencher strand into a 500-μL open-top imaging chamber containing imager at 4 nM. This action yielded a total quencher strand concentration of ~ 15 nM in the chamber and ensured saturated quenching of imager strands. The diffusional distribution of quencher strands in a sample chamber containing fixed cells is fairly rapid and achieved efficient quenching after approximately 5 min (Figs. 4(c) and 4(d)). As shown before, the nonspecific adsorption of imagers is very low in biological samples [14], and as a result, the super-resolution images (e.g., Fig. 4(c)) have very high contrast.

Conventional Exchange-PAINT requires full fluid exchanges from one imager to washing buffer and next imagers. This arrangement is typically achieved either with specially designed chambers [16], which can require complex preparation, or with multiple washing steps in an open-top chamber. A drawback when working with an open chamber is that accidental

full draining can deteriorate sample quality or dislodge the sample.

We demonstrated a full Quencher-Exchange-PAINT cycle in fixed cells by means of an open-top imaging chamber by imaging microtubules and the mitochondrial import receptor subunit TOM20 (Figs. 5(a) and 5(b)). With 1× excess of quencher strands over the imager concentration, efficient suppression of P1+ binding was achieved after 3 min: comparable to the suppression speed shown at the 4× excess above (Figs. 4(c) and 4(d)). The benefits of conventional Exchange-PAINT are preserved, such as negligible crosstalk and independence of chromatic aberrations.

A generalized Quencher-Exchange-PAINT protocol (Fig. 5(c)) implements multiple rounds of Exchange-PAINT without the need for fluid exchange. Here, the sample was imaged in an open-top microscopy chamber, and full suppression of imager binding events could be achieved with a small amount of a concentrated complementary quencher added by pipetting, for example, 1 μL of 500 nM quencher into a 500-μL chamber. This situation should result in a final quencher strand concentration of ~ 1 nM, sufficient to reduce the binding-event rate as well as the background fluorescence to negligible levels. Adding excess quencher strand concentration should speed up the suppression and thus allows for faster switching. Additionally, it guarantees full suppression even in the case of local concentration variations. Note that adding the quencher strand complementary to the previous imager (here P1+) and the subsequent imager (here P2+) at different time points is proposed for quality control, i.e., to check that event rates drop to negligible levels before adding imager complementary to a different docking strand. P1+, P2+, … are orthogonal imagers that follow a scheme similar to the

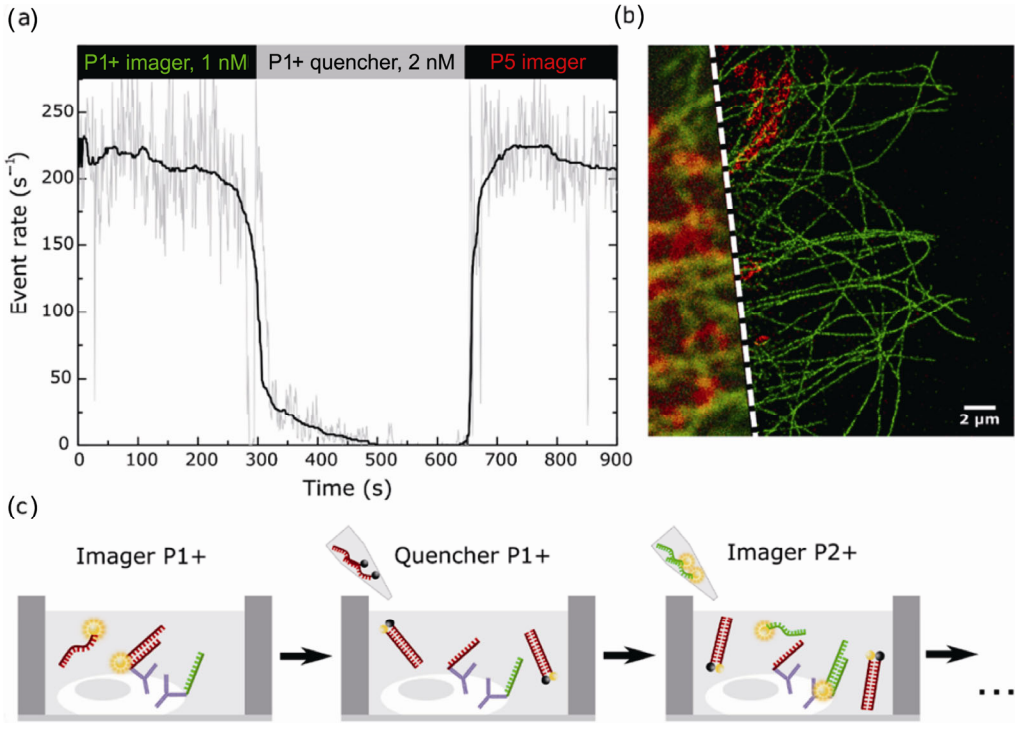

Figure 5 The Quencher-Exchange-PAINT concept involving a simple open-top microscopy chamber. (a) A full Exchange-PAINT cycle using the P1+ imager and quencher for β-tubulin and the P5 imager for TOM20 in fixed COS-7 cells. Low crosstalk is achieved without any washing steps by adding a small amount of the quencher and subsequently the P5 imager into an open chamber. (b) Widefield and rendered Exchange-PAINT image corresponding to data shown in (a), red: TOM20, green: β-tubulin. (c) Left to right: transient binding of imager P1+ to a partially complementary (9 bp) docking strand allows for imaging of the first target. A small volume of highly concentrated complementary (13 bp) quencher strands is added. The concentration is chosen so that the resulting concentration in the chamber is at least equal to the imager concentration. Depending on diffusion, but typically after several minutes, the binding-event rate of the P1+ imager drops to negligible levels, and the imager matching the next target can be added to the sample. In principle, these steps can be repeated with an arbitrary number of orthogonal imager–quencher pairs.

P1+ design presented in Fig. 2, i.e., high affinity between imager and quencher strands, but relatively low affinity between imager and docking strands. This arrangement can be achieved by generalizing the scheme underlying the P1+/P1 strands and adapting it to orthogonal DNA-PAINT strands, such as those evaluated by Jungmann et al. [14]. Even faster and less invasive Quencher-Exchange-PAINT could be achieved by adding the P1+ quencher strand and P2+ imager simultaneously as a mixture at a single pipetting step, and the localization events of suitably chosen transition time are discarded to avoid crosstalk between the P1+ and P2+ channels.

In principle, Quencher-Exchange-PAINT with orthogonal quencher–imager pairs enables multiplexed imaging of an arbitrary number of targets labeled with orthogonal docking strand sequences. Subsequent imager binding (P2+, P3+, …) can be suppressed with respective complementary quencher strands (P2+ quencher, P3+ quencher, …). Repeated imaging and quenching of the same target is possible as well. The free imager concentration $[I] \approx [I_0] - [Q_0]$, which determines the binding-event rate, has to be adjusted by adding sufficient imager, to compensate for an excess quencher strand concentration.

2.5 Rapid imager exchange in Quencher-Exchange-PAINT of tissue samples

In addition to the application of Quencher-Exchange-PAINT to simplified multiplexed super-resolution imaging, we investigated its ability to accelerate imager switching in multiplexed tissue imaging. If the imager solution surrounding the sample is fully replaced by a buffer during a conventional washout, the drop of the event rate depends on the diffusion of imager strands out of the sample. Although these time scales are negligible with DNA origami samples in a free solution and with thin fixed cells, diffusion of imager strands in tissue slices is much more varied and can result in an imager washing step requiring regularly more than 15 min. In our experiments, time scales of 50% removal were as large as 10 min although in some tissue locations in our experiments with murine, rat, and porcine cardiac tissue samples, removal was considerably faster. Notably, there were no obvious criteria to predict imager removal time, and this drawback precluded selecting tissue portions for fast exchange.

Quencher-Exchange-PAINT offers a way to decouple the binding-event rate from the absolute imager concentration and thus from imager diffusion itself (Fig. 6(a)). To reduce the event rate, quencher strands at a concentration much higher (10–50×) than the imager concentration were added to the solution surrounding the tissue. This concentration gradient led to an increase in the quencher strand concentration to a sufficient level throughout the tissue much faster than the diffusion of the imager out of the tissue, resulting in a rapid reduction of the binding-event rate. Figure 6(b) reveals an increasingly rapid event rate suppression with the increasing quencher strand concentrations. Ryanodine receptors in a murine cardiac tissue slice were imaged, and the event rate was modulated sequentially by washing with plain buffer and different concentrations of complementary quencher strands (1, 10, or 50 nM at an initial imager concentration of 1 nM), while the field of view and imaging sequence remained the same for comparability. In the shown case, washing with plain buffer did not decrease the event rate to levels necessary for Exchange-PAINT for over 10 min. Washing with quencher strands 10–50× more concentrated than the imager concentration within the tissue reduced the event rate to background levels within 5 min.

Due to the washing steps involved in the presented tissue Quencher-Exchange-PAINT, the high quencher–imager binding affinity is no longer crucial, because a high proportion of the imager–quencher pairs will be washed out in the process. Therefore, a shorter quencher strand, binding to a conventional P1 imager with a 9 bp overlap, could be used here as well. Nevertheless, the P1+ type approach without explicit solution exchange should also work for tissues, with the following alteration: A larger excess of the P1+ quencher should be added because the acceleration of the suppression of imager-docking binding relies on the saturation of binding between quencher and imager strands. This rapid saturation steepens the time course of reduction in the free imager amount relative to the diffusional time course of the quencher concentration increase.

To demonstrate a full Quencher-Exchange-PAINT cycle in tissue, we imaged porcine and rat cardiac

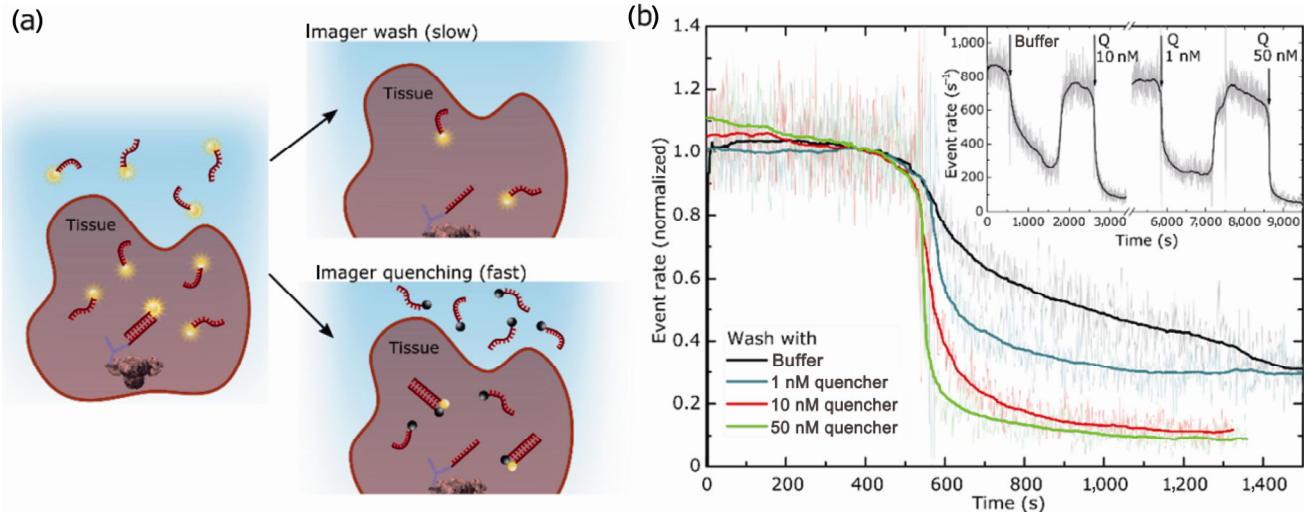

Figure 6 The influence of a fluorescence quencher on washing steps during Exchange-PAINT imaging of cardiac tissue samples. (a) After imaging one target in Exchange-PAINT (left), the imager has to be removed efficiently for subsequent imaging steps. This removal is achieved by replacing the imager with plain buffer (top), but can take several minutes in samples with limited diffusion. Quenching the remaining imager with complementary quencher-conjugated strands will reduce the event rate much more rapidly (bottom). (b) A cardiac tissue sample is washed with plain buffer (black) and increasing quencher concentrations (blue, red, and green), and this approach reduces the event rate more effectively. The inset shows the absolute event rate of the washes; the free imager concentration was readjusted by adding more imager after each wash.

tissue slices, targeting ryanodine receptors (Imager P1) and TOM20 (Imager P3; Fig. 7). The binding-event rate dropped to negligible levels in less than a minute (Fig. 7(a)). Here, the washing step was maintained longer than strictly necessary to demonstrate a constantly low event rate, similar to the background event rate in tissue, after the quencher was added. Subsequent addition of an orthogonal P3 imager allowed for crosstalk-free multiplexed imaging of the next target, here TOM20 (Fig. 7(b)).

3 Conclusions

Here, we introduce Quencher-Exchange-PAINT, which enables rapid, low-crosstalk Exchange-PAINT imaging of protein clusters and membrane structures in cell and tissue samples. The addition of fluorescence quenchers conjugated to oligonucleotides and complementary to imager strands is equivalent to a decrease of imager concentration, reducing both the fluorescence background and the binding-event rate. Thus, exchanging imager solutions in Quencher-Exchange-PAINT can be decoupled from the slow diffusional washout of the residual imager, thereby accelerating the process considerably. The same approach based on quencher-coupled strands can be implemented for straightforward Quencher-Exchange-PAINT imaging without the need for washes and full fluid exchange chambers. The free-imager concentration and therefore the Quencher-DNA-PAINT binding-event rate can be easily tuned by adding a small volume of complementary quencher strands at high concentration into an open-top imaging chamber.

Moreover, we show the flexibility of the synthetic DNA design, by means of an imager and quencher strand pair with slightly extended length that achieves the desired high affinity while not affecting the super-resolution imaging quality. The throughput of Quencher-Exchange-PAINT can in principle be increased by combination with spectrally multiplexed imaging (see Fig. S2 in the ESM). Furthermore, the concept of Quencher-Exchange-PAINT could be used to facilitate other related techniques such as the generalization of Exchange-PAINT to confocal imaging and other super-resolution techniques such as STORM or STED [22–24]. In these methods, a tuning or reduction of the imager-binding rate is also essential and can be facilitated by adding complementary quencher strands.

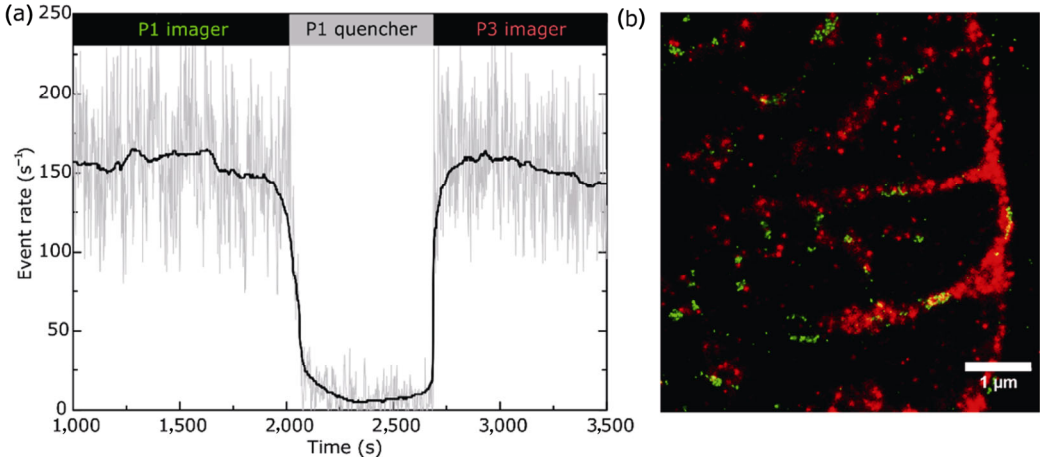

Figure 7 Exchange-PAINT facilitated by a wash with an additional quencher. (a) The DNA PAINT event rate for the P1 imager drops to background levels after a wash with a complementary quencher strand. Subsequently, imager P3 is added. (b) A superimposed image of channels P1 and P3. Green: ryanodine receptors imaged at 1 nM P1, washed with 10 nM P1 quencher. Red: TOM20 imaged with P3 at 1 nM. The tissue slice was imaged 3 µm above the coverslip in HILO mode.

4 Experimental

4.1 Materials and sample preparation

High-performance liquid chromatography (HPLC)-purified modified oligonucleotides were purchased from Eurofins Genomics (Imager strands and streptavidin-modified docking strands for bead experiments, Eurofins Scientific, Luxemburg) and IDT (Amino modified docking strands and quencher modified strands, Integrated DNA Technologies, Coralville). P1 docking strands were labeled with the Cy3 dye to enable quality control via widefield fluorescence imaging. Cy3 excitation at 642 nm is negligible and thus did not interfere with our DNA-PAINT experiments. The sequences used are given in Table 1.

Lyophilized DNA was resuspended and stored in Tris-EDTA (TE, pH 8.0, Sigma-Aldrich) buffer at 100 µM. Dilution in DNA-PAINT buffer (1× PBS, 500 mM NaCl, pH 8.0, see buffer C in Ref. [14]) was carried out for imaging.

Coverslips for imaging of polystyrene (PS) beads were coated with PLL-g-PEG (SuSoS, Duebendorf) to prevent nonspecific binding. PLL-g-PEG at a concentration of 0.1 mg·mL^{-1} in PBS was washed off the coverslip after 30 min. The docking strands were attached to the streptavidin-coated PS beads (diameter: 500 nm, Microparticles GmbH, Berlin) by dispersing them in TE buffer containing 300 mM NaCl and biotinylated docking strands. Docking strands were added in 4× excess concentration as compared to the binding capacity of the beads to ensure a saturated coating. Unbound oligos were removed by repeated centrifugation and redispersion steps.

Table 1 Docking, imager, and quencher strand sequences

Name	Sequence (5′ → 3′)
Permanently binding imager	Atto 647N – TATACATCTATCTTCATTATT – Biotin
Permanently binding quencher	TAATGAAGATAGATGTATT – Iowa Black RQ
P1 imager [14]	CTAGATGTAT – Atto 655
P1 docking	Biotin/antibody – TTATACATCTA – Cy3
P1 quencher	Iowa Black RQ – ATACATCTAC
P1+ imager	GCGCTAGATGTAT – Atto 655
P1+ quencher	Iowa Black RQ – ATACATCTAGCGC
P3 imager [14]	GTAATGAAGA – Atto 655
P3 docking	Biotin/antibody – TTTCTTCATTA
P3 quencher	Iowa Black RQ – TCTTCATTAC
P5 imager [14]	CTTTACCTAA – Atto 655
P5 docking	Antibody – TTTTAGGTAAA

The experimentation with rat and murine tissues was approved by the University of Exeter ethics committee and the use of porcine tissue by the University of Bristol ethics committee. The preparation and immunostaining procedure is described elsewhere in detail [25]. Cryosections were cut at a thickness of 15 µm and deposited onto poly-L-lysine–coated No. 1.5 coverslips. The tissue slices were hydrated, blocked

at room temperature, and then incubated with a primary antibody in an incubation solution (1% BSA; 0.05% Triton X-100; 0.05% NaN_3) at 4 ˚C overnight. All tissue slices were labeled with a ryanodine receptor (RyR) 2–specific antibody, and the rat and pig tissues shown in Fig. 7 were additionally labeled with a primary antibody against the mitochondrial import receptor subunit TOM20. Respective secondary antibodies (Jackson ImmunoResearch, West Grove) conjugated to the DNA-PAINT docking strands were added after multiple washing steps with PBS.

COS-7 cells were seeded on coverslips and grown overnight in DMEM at 37 ˚C and 5% CO_2. After removal of the medium, the cells were fixed in ice-cold methanol for 15 min at –20 ˚C and washed three times in PBS. After that, the cells were permeabilized with 0.2% Triton X-100 in PBS and blocked with 1% BSA in PBS for 10 min each. β-Tubulin and TOM20 were immunostained with respective primary antibodies (1:200 in the incubation solution) at room temperature for 1 h. After three washes with PBS for 5 min each, the respective secondary antibodies conjugated to DNA-PAINT docking strands P1 for β-tubulin and P5 for TOM20 were added at 1% in the incubation solution. The sample was washed three times with PBS for 5 min each before addition of the imager strands.

4.2 Imaging setup

All data were acquired using a modified Nikon Eclipse Ti-E inverted microscope (Nikon, Tokyo) and an Andor Zyla 4.2 sCMOS (scientific complementary metal-oxide-semiconductor) camera (Andor, Belfast). For quality checks of the labeling, a widefield fluorescence imaging LED light source was employed (CoolLED, Andover). Atto 655 was excited with a CW diode laser (Omikron LuxX, Rodgau) at 642 nm with a power of 140 mW, attenuated to approximately 15 mW with an illumination spot with approximately 30 μm diameter in the sample. A 60× 1.49NA APO oil immersion TIRF objective (Nikon, Tokyo) was used. PS beads were imaged in TIRF mode, whereas tissue slices in HILO mode. Thermal drift was reduced with a custom objective holder, and the focus was controlled by a piezo objective scanner (P-725, Physik Instrumente, Karlsruhe). Lateral drift correction during post-analysis was achieved via tracking the data acquired with an auxiliary camera in transmission mode at a non-interfering wavelength. This tracking setup was also implemented for continuous focus stabilization during image acquisition.

4.3 Image acquisition and analysis

Oligo concentrations were estimated by measuring the absorbance at the DNA absorbance peak (260 nm) and at the absorption maximum of the respective dye or quencher oligo modification on a NanoDrop spectrophotometer (Thermo Fisher Scientific, Waltham). Bulk fluorescence was measured in a 200 μL chamber and 50 μm above the coverslip, to minimize the detected fluorescence of imagers adsorbed on the coverslip surface.

DNA-PAINT images were captured with integration time 100 ms. Fluid exchange in Exchange-PAINT experiments on tissue and streptavidin-coated polystyrene beads was facilitated by means of a 3D-printed chamber (printed with Form2, Formlabs, Somerville). It included a straight channel with a volume of approx. 140 μL, an inlet that could be attached to a syringe or a pump (via 0.1″ FEP tubing), and a waste reservoir which was decoupled from the imaging channel. Tissue slices were imaged in HILO mode 5 μm (Fig. 6) and 3 μm (Fig. 7) away from the surface of the coverslip. Fixed cells imaged by Quencher-Exchange-PAINT without the need for washing were imaged in an open-top microscopy chamber. A cleaned coverslip was attached to a reusable Perspex slide with a circular chamber cut in its middle (construction time approx. 1 min, for details see Ref. [26]).

Control of the optical components including the microscope, image acquisition, and analysis was based on a custom-written software package, Python Microscopy Environment (PyME), which is available freely via: https://bitbucket.org/christian_soeller/python-microscopy-exeter/. Single binding events were detected and fitted to a 2D Gaussian for localization. The data were next filtered with respect to parameters of a Gaussian fitting, e.g., the peak intensity, σ and localization errors. Thus, binding events that were not in focus could be effectively suppressed. Drift correction uses data acquired by an auxiliary camera via the transmission light

path, while deviating aberrations between the two imaging paths were corrected for. Super resolution images were rendered by jittered triangulation [27].

Acknowledgements

We thank Rikke Morrish for help with the fixation of COS-7 cells and Anna Meletiou, Cecilia Afonso Rodrigues, Carl Harrison for their help with antibody conjugations and labelling of tissue sections and fixed cells. The authors also acknowledge useful discussions with B.M. Mognetti. The work was supported by funding from the Human Frontier Science Program (No. 0027/2013) and the Engineering and Physical Sciences Research Council of the UK (No. EP/N008235/1).

Electronic Supplementary Material: Supplementary material (theoretical model for the simulation of background fluorescence, further comparison of P1 and P1+ imager strands and a proof-of-principle experiment demonstrating the combination of Quencher-Exchange-PAINT with spectral multiplexing) is available in the online version of this article at https://doi.org/10.1007/s12274-018-1971-6.

References

[1] Huang, B.; Bates, M.; Zhuang, X. W. Super resolution fluorescence microscopy. *Annu. Rev. Biochem.* **2009**, *78*, 993–1016.

[2] Hell, S. W. Microscopy and its focal switch. *Nat. Methods* **2009**, *6*, 24–32.

[3] Bailey, B.; Farkas, D. L.; Taylor, D. L.; Lanni, F. Enhancement of axial resolution in fluorescence microscopy by standing-wave excitation. *Nature* **1993**, *366*, 44–48.

[4] Hell, S.; Stelzer, E. H. K. Properties of a 4Pi confocal fluorescence microscope. *J. Opt. Soc. Am. A* **1992**, *9*, 2159–2166.

[5] Hell, S. W.; Wichmann, J. Breaking the diffraction resolution limit by stimulated emission: Stimulated-emission-depletion fluorescence microscopy. *Opt. lett.* **1994**, *19*, 780–782.

[6] Klar, T. A.; Jakobs, S.; Dyba, M.; Egner, A.; Hell, S. W. Fluorescence microscopy with diffraction resolution barrier broken by stimulated emission. *Proc. Natl. Acad. Sci. USA* **2000**, *97*, 8206–8210.

[7] Betzig, E.; Patterson, G. H.; Sougrat, R.; Lindwasser, O. W.; Olenych, S.; Bonifacino, J. S.; Davidson, M. W.; Lippincott-Schwartz, J.; Hess, H. F. Imaging intracellular fluorescent proteins at nanometer resolution. *Science* **2006**, *313*, 1642–1645.

[8] Hess, S. T.; Girirajan, T. P. K.; Mason, M. D. Ultra-high resolution imaging by fluorescence photoactivation localization microscopy. *Biophys. J.* **2006**, *91*, 4258–4272.

[9] Rust, M. J.; Bates, M.; Zhuang, X. W. Sub-diffraction-limit imaging by stochastic optical reconstruction microscopy (STORM). *Nat. Methods* **2006**, *3*, 793–796.

[10] Heilemann, M.; van de Linde, S.; Schüttpelz, M.; Kasper, R.; Seefeldt, B.; Mukherjee, A.; Tinnefeld, P.; Sauer, M. Subdiffraction-resolution fluorescence imaging with conventional fluorescent probes. *Angew. Chem., Int. Ed.* **2008**, *47*, 6172–6176.

[11] Legant, W. R.; Shao, L.; Grimm, J. B.; Brown, T. A.; Milkie, D. E.; Avants, B. B.; Lavis, L. D.; Betzig, E. High-density three-dimensional localization microscopy across large volumes. *Nat. Methods* **2016**, *13*, 359–365.

[12] Curdt, F.; Herr, S. J.; Lutz, T.; Schmidt, R.; Engelhardt, J.; Sahl, S. J.; Hell, S. W. isoSTED nanoscopy with intrinsic beam alignment. *Opt. Express* **2015**, *23*, 30891–30903.

[13] Sharonov, A.; Hochstrasser, R. M. Wide-field subdiffraction imaging by accumulated binding of diffusing probes. *Proc. Natl. Acad. Sci. USA* **2006**, *103*, 18911–18916.

[14] Jungmann, R.; Avendaño, M. S.; Woehrstein, J. B.; Dai, M. J.; Shih, W. M.; Yin, P. Multiplexed 3D cellular super-resolution imaging with DNA-PAINT and Exchange-PAINT. *Nat. Methods* **2014**, *11*, 313–318.

[15] Jungmann, R.; Steinhauer, C.; Scheible, M.; Kuzyk, A.; Tinnefeld, P.; Simmel, F. C. Single-molecule kinetics and super-resolution microscopy by fluorescence imaging of transient binding on DNA origami. *Nano Lett.* **2010**, *10*, 4756–4761.

[16] Schnitzbauer, J.; Strauss, M. T.; Schlichthaerle, T.; Schueder, F.; Jungmann, R. Super-resolution microscopy with DNA-PAINT. *Nat. Protoc.* **2017**, *12*, 1198–1228.

[17] Agasti, S. S.; Wang, Y.; Schueder, F.; Sukumar, A.; Jungmann, R.; Yin, P. DNA-barcoded labeling probes for highly multiplexed exchange-PAINT imaging. *Chem. Sci.* **2017**, *8*, 3080–3091.

[18] Thompson, R. E.; Larson, D. R.; Webb, W. W. Precise nanometer localization analysis for individual fluorescent probes. *Biophys. J.* **2002**, *82*, 2775–2783.

[19] Markham, N. R.; Zuker, M. DINAMelt web server for nucleic acid melting prediction. *Nucleic Acids Res.* **2005**, *33*, W577–W581.

[20] Markham, N. R.; Zuker, M. UNAFold: Software for nucleic acid folding and hybridization. In *Bioinformatics, Volume II. Structure, Function and Applications*. Keith, J. M., Ed.; Humana Press: Totowa, NJ, 2008; pp 3–31.

[21] Molle, J.; Raab, M.; Holzmeister, S.; Schmitt-Monreal, D.; Grohmann, D.; He, Z. K.; Tinnefeld, P. Superresolution microscopy with transient binding. *Curr. Opin. Biotechnol.* **2016**, *39*, 8–16.

[22] Schueder, F.; Strauss, M. T.; Hoerl, D.; Schnitzbauer, J.; Schlichthaerle, T.; Strauss, S.; Yin, P.; Harz, H.; Leonhardt, H.; Jungmann, R. Universal super-resolution multiplexing by DNA exchange. *Angew. Chem., Int. Ed.* **2017**, *56*, 4052–4055.

[23] Wang, Y.; Woehrstein, J. B.; Donoghue, N.; Dai, M. J.; Avendaño, M. S.; Schackmann, R. C. J.; Zoeller, J. J.; Wang, S. S. H.; Tillberg, P. W.; Park, D. et al. Rapid sequential *in situ* multiplexing with DNA exchange imaging in neuronal cells and tissues. *Nano Lett.* **2017**, *17*, 6131–6139.

[24] Beater, S.; Holzmeister, P.; Lalkens, B.; Tinnefeld, P. Simple and aberration-free 4color-STED-multiplexing by transient binding. *Opt. Express* **2015**, *23*, 8630–8638.

[25] Hou, Y. F.; Crossman, D. J.; Rajagopal, V.; Baddeley, D.; Jayasinghe, I.; Soeller, C. Super-resolution fluorescence imaging to study cardiac biophysics: α-actinin distribution and Z-disk topologies in optically thick cardiac tissue slices. *Prog. Biophys. Mol. Biol.* **2014**, *115*, 328–339.

[26] Crossman, D. J.; Hou, Y. F.; Jayasinghe, I.; Baddeley, D.; Soeller, C. Combining confocal and single molecule localisation microscopy: A correlative approach to multi-scale tissue imaging. *Methods* **2015**, *88*, 98–108.

[27] Baddeley, D.; Cannell, M. B.; Soeller, C. Visualization of localization microscopy data. *Microsc. Microanal.* **2010**, *16*, 64–72.